Published in final edited form as:
Nature. 2007 June 14; 447(7146): 869–874. doi:10.1038/nature05877.

Resolvin E1 and Protectin D1 Activate Inflammation-Resolution Programs

Jan M. Schwab[*,1], **Nan Chiang**[*], **Makoto Arita**[2], and **Charles N. Serhan**[§]
Center for Experimental Therapeutics and Reperfusion Injury, Department of Anesthesiology, Perioperative and Pain Medicine, Brigham and Women's Hospital and Harvard Medical School, Boston, MA, USA

Abstract

Resolution of acute inflammation is an active process essential for appropriate host responses, tissue protection and the return to homeostasis[1-3]. During resolution, specific omega-3 polyunsaturated fatty acid (PUFA)-derived mediators are generated within resolving exudates, including resolvin E1 (RvE1)[4] and protectin D1 (PD1)[5]. It was deemed important to pinpoint specific actions of RvE1 and PD1 in regulating tissue resolution. Here we report RvE1 and PD1 at nanogram ranges promote phagocyte removal during acute inflammation, via regulating leukocyte infiltration, increasing macrophage ingestion of apoptotic PMNs *in vivo* and *in vitro*, and enhancing the appearance of phagocytes carrying engulfed zymosan in lymph nodes and spleen. In this tissue terrain, inhibition of either cyclooxygenase or lipoxygenases, pivotal enzymes in the temporal generation of both pro-inflammatory and pro-resolving mediators, caused a “resolution deficit” that was rescued by RvE1, PD1 or aspirin-triggered lipoxin A_4 analog (ATLa). Also, new resolution routes were identified that involve phagocytes traversing perinodal adipose tissues and non-apoptotic PMNs carrying engulfed zymosan to lymph nodes. Together, these results identify new active components for post-exudate resolution traffic, and demonstrate that RvE1 and PD1 are potent agonists for resolution of inflamed tissues.

Acute local inflammation in healthy individuals is self-limited and resolves via an active termination program[1,2]. Specialized chemical mediators are generated in this biochemically active process[4-7]. Their complete stereochemical assignments were recently established and organic syntheses achieved[8-10]. These include arachidonic acid-derived lipoxin A_4 (LXA_4) and its epimer ATL[8], eicosapentaenoic acid (EPA)-derived RvE1[4,9], and docosahexaenoic acid (DHA)-derived PD1/neuroprotectin D1[5,10,11] (Fig. 1). Recently, we assembled a “resolution map” using lipidomics and proteomics to identify major cellular/molecular components, and introduced quantitative resolution indices[12] (Supplemental Fig. 1). Each of these endogenous mediators elicits specific actions within resolution circuitry, giving precise quantitative changes in resolution indices[12].

The key histological event in tissue resolution is the loss of inflammatory PMN[13]. In a spontaneous resolving zymosan-initiated peritonitis, total leukocyte infiltration reached maximal at ~12h, and by 24h reduced ~50%[12]. Hence, 24h post-zymosan is well within the

Correspondence: Prof. Charles N. Serhan, Director, Center for Experimental Therapeutics and Reperfusion Injury, Department of Anesthesiology, Perioperative and Pain Medicine, Brigham and Women's Hospital and Harvard Medical School, Boston, MA 02115. Phone: 617-732-8822; Fax: 617-582-6141. E-mail: cnserhan@zeus.bwh.harvard.edu.
[*]These authors contributed equally to this work
[1]Present address: Klinik und Poliklinik für Neurologie & Experimentelle Neurologie, Campus-Mitte, Charité Universitätsmedizin Berlin, Charitéplatz 1, 10117 Berlin, Germany
[2]Present address: Department of Health Chemistry, Graduate School of Pharmaceutical Sciences, University of Tokyo, 7-3-1 Hongo, Bunkyo-ku, Tokyo 113-0033, Japan

classic resolution phase, and was selected to study the impact of RvE1 and PD1. When given together with zymosan, PD1 (300 ng, ip) dramatically reduced PMN infiltration by >40%, compared to mice challenged with zymosan ($6.7\pm0.1x10^6$ vs.$11.6\pm1.0x10^6$ PMN), illustrating potent anti-inflammation (Fig. 1A, *left*). For comparison, equi-doses of ATLa gave ~26% PMN reduction, and RvE1 increased mononuclear infiltrates ~24%. These results indicate that each family of resolving mediators differentially impacts exudate cellular composition. When ATLa, RvE1 and PD1 were given at the peak of inflammation (12h after zymosan injection), each retained the ability to reduce PMN numbers at 24h (Fig. 1A, right) and gave similar resolution intervals (Fig. 1B), demonstrating their potent pro-resolving actions.

Inflammation-resolution is a dynamic process, with cells being recruited (influx) and cleared from (efflux) local inflamed sites. Reduction in exudate cells by these mediators may reflect their actions on anti-inflammation (reducing cell recruitment) versus pro-resolution (enhancing cell exit), or both. Hence, it was important to determine whether these mediators directly activate specific resolution programs. We evaluated whether RvE1 and PD1 impact macrophage ingestion of apoptotic PMNs *in vivo*, an essential part of the resolution orchestra in tissues[14] (Fig. 2A). ATLa and PD1-treated mice showed increased macrophages with ingested PMN ($F4/80^+Gr\text{-}1^+$), and thus enhanced phagocytosis at 24h (Fig. 2A). ATLa, RvE1 or PD1 did not directly stimulate PMN apoptosis *in vivo* when given either at the initiation or peak of inflammation (Supplemental Fig. 2). Cyclin-dependent kinase and specific ERK1/2 inhibitors, in comparison, given at the peak of inflammation enhance resolution by promoting PMN apoptosis[15,16], via a different mechanism than PUFA-derived endogenous mediators.

We also examined phagocytosis *in vitro*. Coincubation of elicited macrophages with apoptotic PMN induced endogenous LXA_4 generation (Fig. 2B, *inset*), but not pro-inflammatory leukotriene B_4. LXA_4 peaked at 15 min during coincubations [20.7±2.6 pg/0.2 ml, ~280 nM], identified by diagnostic ions in its MS/MS spectrum (Fig. 2B). Macrophage phagocytosis was also apparent at 15 min and gradually increased until 2h. These findings indicated that apoptotic PMNs, when ingested by macrophages, rapidly initiated LXA_4 formation, which likely contributes to enhanced macrophage phagocytosis[17] at later intervals (30-120 min). Apoptotic Jurket cells also stimulate LXA_4 during macrophage phagocytosis[18]. Of interest, during phagocytosis, PD1 was generated (23.2±2.1 pg/ml; ~ 70 nM), monitored by LC/MS/MS (Supplemental Fig. 3). RvE1 was also formed by isolated cells with aspirin (~ 6 pg/ml, ~16 nM), and this level increased (~11 pg/ml, ~30 nM) with substrate EPA (Fig. 2B, MS/MS spectrum in Supplemental Fig. 3). Thus, LXA_4, RvE1 and PD1 are produced when macrophages phagocytoze apoptotic PMN.

To investigate whether this set of pro-resolving mediators have a direct impact on isolated macrophages, macrophages were exposed to LXA_4, RvE1 or PD1 (100 nM) prior to apoptotic PMN. Approximately 40% of macrophages ingested PMN ($F4/80^+Gr\text{-}1^+$) at 60 min with vehicle alone. RvE1 and PD1 each enhanced $F4/80^+Gr\text{-}1^+$ macrophages 36±5% and 44±10%, respectively, compared to vehicle (Fig. 2C). LXA_4 increased $F4/80^+Gr\text{-}1^+$ macrophages ~20%, in line with earlier findings[17]. LXA_4, RvE1 and PD1 each regulated release of chemokine/cytokine during phagocytosis, reducing IFN-γ and IL-6 (Fig. 2C). In addition, LXA_4 increased anti-inflammatory IL-10. There were no apparent changes in TNF-α, KC, JE and MIP-2 (Supplemental Fig. 4). These results indicated RvE1 and PD1 each promoted non-phlogistic macrophage engulfment of apoptotic PMN. Taken together, it is now evident that LXA_4, RvE1 and PD1 were generated *in vitro* (within 60 min) during macrophage-apoptotic PMN interactions (Fig. 2B). In turn, when macrophages were exposed to these mediators (20 min), they stimulated ingestion of apoptotic PMN (Fig. 2C). Glucocorticoid-stimulated phagocytosis of apoptotic PMN requires much longer intervals (3-24h) by comparison, and involves annexin I generation[19,20]. The process of macrophage ingestion of apoptotic PMN was recently coined “efferocytosis”[21]

Zymosan recognition models that of microbes by the innate immune system[22]. LXA_4, RvE1 or PD1 (100 nM), incubated with macrophages, stimulated uptake of zymosan 93±7%, 95 ±27%, and 119±20%, respectively, compared to vehicle (Fig. 2D). These mediators also enhanced macrophage uptake of non-opsonized latex beads, albeit to a much lesser extent (Fig. 2D). Thus, in addition to apoptotic PMNs, LXA_4, RvE1 and PD1 are potent stimulators of macrophage uptake of microbial particles, i.e., opsonized zymosan.

We questioned whether these resolution agonists impact leukocyte traffic from zymosan-inflamed peritoneum via lymph nodes (LN) and spleen. In the resolution phase (24h), the most pronounced locations of phagocytes carrying ingested zymosan (i.e. leukocytes with engulfed zymosan, zymosan^e leukocytes) were in the outer cortex of LN (Fig. 3Aa), and in spleen within the marginal zone surrounding white pulp (Fig. 3Ab). ATLa (300 ng) increased zymosan^e leukocytes in LN at 24h (Fig. 3A), giving >2-fold increase of total zymosan (0.23±0.03 vs. 0.09±0.04 μg zymosan/μg protein in mice given zymosan alone) (Fig. 3B). Significant increases in zymosan levels in spleens were also observed. Passive efflux of non-engulfed zymosan was excluded, since significant extracellular association of zymosan was not apparent. Thus, total zymosan levels represent phagocytic leukocytes within LN and spleen. RvE1 also enhanced zymosan^e leukocytes in both LN and spleen, with modest increases in LN, compared to significant increases in the spleen. PD1-treated mice gave dramatic increases in zymosan levels >6-fold in LN and >4-fold in the spleen. When ATLa, RvE1 or PD1 were each given at the peak of inflammation, they also enhanced, to a lesser extent, zymosan^e leukocytes in LN and spleen (Fig. 3B). Thus, LXA_4, RvE1 and PD1 are biosynthesized in inflammatory exudates[12] (Supplemental Fig. 5), and when these mediators were added back, they promoted phagocyte removal of microbial challenge via lymphatics. It is noteworthy that their precursors (AA, EPA and DHA) were also elevated during peritonitis[12] (Supplemental Fig. 5).

Next, we investigated whether disruption of biosynthetic pathways of these mediators altered resolution. In the aspirin-triggered biosynthesis of ATL and RvE1, acetylated cyclooxygenase (COX)-2 is pivotal[4,8] (Supplemental Fig. 6). Pharmacologic inhibition of COX-2 delays resolution[23]. In peritoneal leukocytes, COX-2 was induced within 4h after zymosan challenge and remained elevated until 72h (not shown). COX-2 inhibition by NS-398 (10 μM) decreased macrophage phagocytosis of apoptotic PMNs *in vitro*, and reduced PGE_2 and LXA_4 (Supplemental Fig. 7). Lipoxygenases (LOX) are also essential in biosynthesis of PUFA-derived mediators[4,5,8,24]. LOX inhibition by baicalein[25] (10 μM) impaired macrophage phagocytosis, and reduced LXA_4, 15- and 12-HETE, as well as 17-HDHA, a marker of PD1 biosynthesis (Supplemental Fig. 7). Thus, reduction in protective mediators (e.g. LXA_4) may reflect hampered phagocytosis when COX and LOX inhibitors were present.

During peritonitis, COX inhibition by NS-398[23] (100 μg) increased exudate leukocytes ~22% and PMNs ~41% at 24h (Fig. 3C and Supplemental Table 1). Additionally, zymosan amounts in both LN and spleen were significantly reduced >50%, indicating impaired resolution. When ATLa, RvE1 or PD1 (300 ng) was administered along with COX-2 inhibitor, each markedly reduced exudate leukocytes and increased zymosan amounts in lymphatics to levels comparable to those in zymosan-challenged mice (Fig. 3C). The LOX inhibitor (100 μg) gave similar results (Fig. 3D and Supplemental Table 1). Hence, disrupting biosynthesis of these protective mediators with either COX-2 or LOX inhibitors caused a “resolution deficit” phenotype, blocking phagocytic removal of microbial challenge, thereby delaying resolution. These results emphasize a pivotal homeostatic role for COX-2[23] and LOX[24] in resolution of acute inflammation. Importantly, pro-resolving mediators at much lower doses (by at least 2 log orders) rescued defective resolution caused by these pharmacological interventions.

To further study phagocytes exiting the inflamed peritoneum, mice were injected with FITC-labelled zymosan. As early as 4h, we found leukocytes carrying FITC-zymosan (FITC-zymosan^e leukocytes) appearing first in the perinodal adipose tissue (12±5 FITC-zymosan^e leukocytes/high power field [HPF], Fig. 4A and 4Biii-vi), indicating that exiting leukocyte traffic from the inflamed site started early, namely during the acute inflammatory phase. In contrast, few FITC-zymosan^e leukocytes were noted in LN, and none apparent in spleen. With progression of resolution at 24h, FITC-zymosan^e leukocytes increased >2-fold in perinodal adipose tissue, with the highest numbers in LN (~50 FITC-zymosan^e leukocytes/HPF), and also appeared within the spleen. In LN, a small population of FITC-zymosan^e leukocytes observed within cortex areas were PMN (~10%) (Fig. 4Bvii-ix), indicating that these PMNs were phagocytically active, directly transported zymosan to LN prior to their apoptosis and later engulfment by macrophages. Some of the FITC-zymosan^e leukocytes displayed dendritic cell-like morphology with characteristic fine cellular protrusions within afferent lymph vessels (Fig. 4Bx) and spleen (Fig. 4Bxi, xii).

The widely appreciated exit routes of leukocytes from inflamed peritoneum involve drainage via afferent lymph vessels into LN (lymphatic) and subsequently into the spleen (humoral)[13] (Supplemental Fig 9). We identified, in addition to these, high numbers of FITC-zymosan^e leukocytes extravasating from the afferent lymph vessels into perinodal adipose tissue before reaching LN (subcapsular sinus; Fig. 4Biii-vi). We coined this process “lipopassage”, because it is a new trafficking route for leukocytes to exit exudates. Macrophage efflux from the peritoneum into lymphatics is dependent on different adhesion molecules, such as beta1-integrin[26] and Mac-1 (CD11b/CD18)[27]. CD18 is involved in LXA_4-stimulated macrophage phagocytosis of apoptotic PMN[17]. Hence, it is likely that adhesion molecules play a role in lipopassage. Adipocytes are anatomically associated with LN and may be involved in modulating inflammation[28]. Our present findings provide a potential link between perinodal adipose tissue and phagocyte removal from exudates during resolution. In addition, non-apoptotic PMNs carrying zymosan exit exudates, providing evidence that PMNs themselves actively contribute to resolution of inflammation, along with macrophages. Thus, disease processes recently linked to inflammation (e.g. diabetes and obesity)[29] may involve resolution deficits as part of their pathogenesis.

Here, we demonstrate novel protective actions for RvE1 and PD1 in promoting resolution following microbial challenge, as evidenced by: a) regulating leukocyte infiltration, b) stimulating macrophage phagocytosis of apoptotic PMNs, and c) increasing phagocytes carrying zymosan in LN and spleen (Supplemental Fig. 10). These potent “resolution agonists” orchestrate the return of the tissue to homeostasis and are able to rescue resolution deficits inplaced by pharmacological inhibitors of COX and LOX. Together, these results emphasize that resolution agonists (e.g. RvE1 and PD1) and resolution programs may have therapeutic potential when sustained inflammation and/or impaired resolution are components of pathophysiology.

Method Summary

Murine peritonitis

FVB mice were given lipid mediators (300 ng) along with or 12h after zymosan A (1 mg/ml) by intraperitoneal injection. COX-2 inhibitor (NS-398) or LOX inhibitor (baicalein) was each given (100 μg) 30 min before zymosan challenge.

Phagocytosis and apoptosis

For PMN apoptosis, exudate cells were labeled with FITC-conjugated anti-annexin-V Ab and PE-conjugated anti-mouse Gr-1 Ab. For phagocytosis *in vivo*, exudate cells were labelled with

FITC-conjugated anti-mouse F4/80 Ab, permeabilized with 0.1 % Triton X-100, and then labelled with PE-anti-Gr-1 Ab. For phagocytosis *in vitro*, aged PMNs were labeled with PE-anti-Gr-1 Ab. Elicited macrophages were incubated with lipid mediators. PE-anti-Gr-1 Ab-labeled PMNs were then coincubated with treated macrophages at a 2:1 ratio. In separate experiments, fluorescent-labeled zymosan or latex particles were added to treated macrophages at a 10:1 ratio. Macrophages were then labeled with FITC-anti-F4/80 Ab, and monitored by flow cytometry.

Mediator lipidomics

Mass spectral analyses were performed using a Qstar XL equipped with a Turbospray ion source and operated in negative electrospray mode.

Zymosan quantitation by ELISA

Inguinal lymph nodes and spleens from zymosan-injected mice were harvested, zymosan extracted by homogenization and sonication, and supernatants collected. For competitive ELISA assay, 96-well plates were pre-coated with anti-zymosan IgG, followed by addition of FITC-zymosan and supernatants containing zymosan. Fluorescence was monitored by fluorometry.

Immunohistochemistry

Immunohistology slides prepared from paraffin-embedded sections were incubated with either rabbit anti-zymosan Ab or rabbit anti-FITC Ab, followed by biotinylated swine anti-rabbit IgG, and peroxidase-conjugated streptavidin-biotin complex. The bound peroxidase was visualized with diaminobenzidine (brown precipitate). Zymosan-containing cells were determined by counting in 10 high-power fields (200x).

Statistics

Results are expressed as mean ± SEM. Group comparisons were carried out using one-way ANOVA or Student's *t*-test, with P values ≤ 0.05 taken as statistically significant.

Methods

Murine peritonitis

Male FVB mice (6-8 weeks; Charles River, Wilmington, MA) were anesthetized with isoflurane. Zymosan A (1 mg/ml, Sigma, St Louis, MO) was administered intraperitoneally alone or with specific lipid mediators (i.e. ATLa, RvE1, PD1, 300 ng/mouse or ~12 μg/kg, i.p.) for these experiments. In separate groups, ATLa, RvE1 or PD1 was given 12h after zymosan injection. ATLa, RvE1 and PD1 were prepared by total organic synthesis in the Organic Synthesis Core (P50-DE016191)[8-10] in accordance with recently published physical and biological criteria. In the case of COX-2 inhibitor (NS-398, from Cayman Chemicals, Ann Arbor, MI) and LOX inhibitor (baicalein, from Sigma, St. Louis, MO), each was given at 100 μg/mouse (or ~4 mg/kg) 30 min before zymosan challenge. At indicated time intervals, mice were euthanized with an overdose of isoflurane, peritoneal exudate cells collected, and differential leukocyte counts determined. All animal procedures were conducted in accordance with the Harvard Medical Area Standing Committee on Animals (protocol no. 02570).

FACS analysis for phagocytosis and apoptosis

For determining macrophage ingestion of PMN *in vivo*, cells were first blocked with anti-mouse CD16/32 blocking Ab (0.5 μg Ab/0.5x106 cells, eBioscience, San Diego, CA) for 5 min, labelled with FITC-conjugated anti-mouse F4/80 Ab (0.5 μg Ab/0.5x106 cells, eBioscience) for 20 min, and permeabilized with 0.1 % Triton X-100 (100 μl, 10 min). Subsequently,

permeabilized cells were labelled with PE-conjugated anti-mouse Gr-1 (Ly-6G) Ab (0.5 μg Ab/0.5x106 cells, eBioscience) for 20 min. The $F4/80^{+}Gr\text{-}1^{+}$ macrophage population was determined by FACS analysis.

For determining PMN apoptosis *in vivo*, exudate cells were labeled with FITC-conjugated anti-annexin-V Ab (0.5 μg Ab/$0.5x10^{6}$ cells, eBioscience) PE-conjugated anti-mouse Gr-1 (Ly-6G) Ab (0.5 μg Ab/$0.5x10^{6}$ cells, eBioscience) for 20 min. The annexin-$V^{+}Gr\text{-}1^{+}$ PMN population was monitored by FACS.

For determining macrophage phagocytosis of apoptotic PMN *in vitro*, murine peritoneal PMN were collected after 4 h peritonitis, aged for 24 h in culture in complete RPMI (BioWhittaker, Watersville, MD), and then labeled with PE-conjugated anti-mouse Gr-1 Ab. Elicited macrophages were collected after 72 h peritonitis and incubated with lipid mediators (i.e. LXA_4, RvE1, PD1, 100 nM) or vehicle alone for 20 min. LXA_4 was from Calbiochem (San Diego, CA). PE-Gr-1 Ab-labeled apoptotic PMNs were then coincubated with previously treated macrophages at a 2:1 ratio for the time indicated. Finally, macrophages were labeled with FITC-conjugated anti-mouse F4/80 Ab, and $F4/80^{+}Gr\text{-}1^{+}$ macrophages were evaluated using FACsort software gated for 10,000 events.

For determining macrophage phagocytosis of zymosan (Texas Red-labelled, Molecular Probes) or latex (Fluo Spheres® Carboxylate-modified microspheres, 1.0 μm, orange fluorescent; Molecular Probes), elicited macrophages were collected after 72 h peritonitis and incubated with lipid mediators (i.e. LXA_4, RvE1, PD1, 100 nM) or vehicle alone for 20 min. Zymosan or latex particles were then incubated with previously treated macrophages at a 10:1 ratio for 60 min. Macrophages were collected and labelled with FITC-conjugated anti-mouse F4/80 Ab. $F4/80^{+}zymosan^{+}$ or $F4/80^{+}latex^{+}$ macrophages were evaluated using FACsort software gated for 10,000 events.

Mediator lipidomics

Samples were extracted with deuterium-labeled internal standards [1-2 ng of deuterium-labeled PGE_2 and 0.4 ng of deuterium-labeled PD1] using C18 solid phase extraction (Alltech Associates, Deerfield, IL). For LC/MS/MS analysis, an Applied Biosystems (Foster City, CA) Qstar XL was used, equipped with a LUNA C18-2 (100 x 2 mm x 5 μm) column. HPLC conditions: 0-8 min, 50% A, 50% B; 8-30min, 100% B [A: 0.01% acetic acid, B: acetonitrile:methanol:acetic acid 50:50:0.01%], flow rate 0.2ml/min, UV 190 to 400 nm. All mass spectral analyses were performed using a Qstar XL equipped with a Turbospray ion source and operated in negative electrospray mode. Parameters for TOF mass scan and product ion scans were: Cur=30 p.s.i., GS1=40 p.s.i., GS2=50 p.s.i., CAD 5, TEM= 400°C. DP=-50V, FP=-220, DP2=-10, ISV=-4200. Q1 resolution unit. The voltage used for collisional activated dissociation varied according to molecular species and ranged from -20 to -30V for product ion scan. A mixture of synthetic 15-, 12-, 5-HETE, LXA_4, RvE1, 17S-HDHA and PD1 was used to obtain standard curves for each compound. Linear regression gave R-square values of >0.99 for each. In some experiments, LXA_4 and LTB_4 formation was also determined by ELISA (Neogen, Lexington, KY).

Quantitation of zymosan A particles

Inguinal lymph nodes and spleens were collected (24 h after zymosan injection), and dried in an oven (60°C). Dried tissues were pulverized mechanically, resuspended in 50 mM PBS with 1% Triton-X, and homogenized, followed by sonication and three cycles of freeze-thaw. Samples were centrifuged, supernatants collected and total protein amounts determined using Bio-Rad protein assay (Bio-Rad, Hercules, CA).

ELISA procedure—Polystyrene 96-well plates were pre-coated with rabbit anti-zymosan IgG (1 mg/well, Molecular Probes, Eugene, OR). The competitive ELISA assay was initiated by adding FITC-zymosan (0.5 μg/50 μl), together with either zymosan standards (serial dilutions from 1 to 200 μg/ml) or samples (50 μl) into each well. After incubation for 2h at RT and three washings with wash buffer, 200μl of ELISA buffer was added to each well. Fluorescence was then determined by a fluorometer. All samples were assayed in triplicate, and zymosan levels were normalized by either dry tissue weight or total protein amounts in each sample.

Immunohistochemistry

Inguinal lymph nodes, corresponding afferent lymph vessels, and perinodal adipose tissues were excised 4 and 24 h following zymosan or FITC-zymosan challenge. Slides for immunohistology were prepared for a service fee by the Specialized Histopathology Core Laboratory, Department of Pathology, Brigham and Women's Hospital, Boston, USA. After formaldehyde fixation and paraffin-embedding, sections were incubated with the primary rabbit anti-zymosan Ab (Molecular Probes, Eugene, OR, 1:500) or rabbit anti-FITC Ab (Dako, Carpenteria, CA) overnight at 4° C. Specific binding of the Ab was detected with a secondary biotinylated swine anti-rabbit IgG $F(ab)_2$ fragment (1:400, 30 min, Dako), followed by incubation with a peroxidase-conjugated streptavidin-biotin complex (Dako). The bound peroxidase was then visualized with diaminobenzidine as a chromogen (brown precipitate). Sections were counterstained with Mayer's Hemalaun. Negative controls consisted of sections incubated in the absence of the primary Ab. The number of cells with engulfed FITC-zymosan in the perinodal adipose tissue, lymph nodes, and spleen was determined by counting in 10 high-power fields [HPF] (200x magnification).

Statistics

All results were calculated and expressed as mean ± standard error of mean (mean ± SEM). Group comparisons were carried out using one-way ANOVA or Student's *t*-test where appropriate, with P values ≤ 0.05 taken as statistically significant (sufficient to reject the null hypothesis).

Supplementary Information

Refer to Web version on PubMed Central for supplementary material.

Acknowledgments

These studies were supported in part by NIH grants GM 38765, P50-DE016191, DK074448 (CNS), and the German Research Council (DFG, Schw 1064/1-1) (JMS). We thank Dr Jeffrey Kutok, M.D., Ph.D. (Dept. of Pathology, BWH and Harvard Medical School) for helpful discussion regarding immunohistology, Gabrielle Fredman for expert assistance with FACS and Siva Elangovan for technical support. We also thank Dr. Ling Xu and Katherine Gotlinger for mass spectral analyses and Mary Small for manuscript preparation.

Abbreviations

AA
: arachidonic acid

ATL
: aspirin-triggered lipoxin A_4 [5*S*, 6*R*, 15*R*-trihydroxyl-7,9,13-*trans*-11-*cis*-eicosatetraenoic acid]

DHA
: docosahexaenoic acid

EPA
: eicosapentaenoic acid

LXA_4
: lipoxin A_4 [5*S*, 6*R*, 15*S*-trihydroxyl-7,9,13-*trans*-11-*cis*-eicosatetraenoic acid]

PD1
: protectin D1/*neuro*protectin D1 [10*R*,17*S*-dihydroxy-docosa-4*Z*,7*Z*,11*E*,13*E*, 15*Z*,19*Z*-hexaenoic acid]

PUFA
: polyunsaturated fatty acids

RvE1
: resolvin E1 [5*S*,12*R*,18*R*-trihydroxy-6*Z*,8*E*,10*E*,14*Z*,16*E*-eicosapentaenoic acid

References

1. Serhan CN, Savill J. Resolution of inflammation: the beginning programs the end. Nat Immunol 2005;6:1191–1197. [PubMed: 16369558]
2. Gilroy DW, Lawrence T, Perretti M, Rossi AG. Inflammatory resolution: new opportunities for drug discovery. Nat Rev Drug Discov 2004;3:401–416. [PubMed: 15136788]
3. Nathan C. Points of control in inflammation. Nature 2002;420:846–852. [PubMed: 12490957]
4. Serhan CN, et al. Novel functional sets of lipid-derived mediators with antiinflammatory actions generated from omega-3 fatty acids via cyclooxygenase 2-nonsteroidal antiinflammatory drugs and transcellular processing. J Exp Med 2000;192:1197–1204. [PubMed: 11034610]
5. Hong S, Gronert K, Devchand P, Moussignac R-L, Serhan CN. Novel docosatrienes and 17S-resolvins generated from docosahexaenoic acid in murine brain, human blood and glial cells: autacoids in anti-inflammation. J Biol Chem 2003;278:14677–14687. [PubMed: 12590139]
6. Levy BD, Clish CB, Schmidt B, Gronert K, Serhan CN. Lipid mediator class switching during acute inflammation: signals in resolution. Nature Immunol 2001;2:612–619. [PubMed: 11429545]
7. Maddox JF, Serhan CN. Lipoxin A_4 and B_4 are potent stimuli for human monocyte migration and adhesion: selective inactivation by dehydrogenation and reduction. J Exp Med 1996;183:137–146. [PubMed: 8551217]
8. Serhan, CN., guest-editor. Prostaglandins Leukot Essent Fatty Acids. Vol. 73. 2005. Special Issue on Lipoxins and Aspirin-Triggered Lipoxins; p. 139-321.
9. Arita M, et al. Stereochemical assignment, anti-inflammatory properties, and receptor for the omega-3 lipid mediator resolvin E1. J Exp Med 2005;201:713–722. [PubMed: 15753205]
10. Serhan CN, et al. Anti-inflammatory actions of neuroprotectin D1/protectin D1 and its natural stereoisomers: assignments of dihydroxy-containing docosatrienes. J Immunol 2006;176:1848–1859. [PubMed: 16424216]
11. Bazan NG. Cell survival matters: docosahexaenoic acid signaling, neuroprotection and photoreceptors. Trends Neurosci 2006;29:263–271. [PubMed: 16580739]
12. Bannenberg GL, et al. Molecular circuits of resolution: Formation and actions of resolvins and protectins. J Immunol 2005;174:4345–4355. [PubMed: 15778399]
13. Cotran, RS.; Kumar, V.; Collins, T., editors. Robbins Pathologic Basis of Disease. W.B. Saunders Co.; Philadelphia: 1999.
14. Savill J, Dransfield I, Gregory C, Haslett C. A blast from the past: clearance of apoptotic cells regulates immune responses. Nat Rev Immunol 2002;2:965–75. [PubMed: 12461569]
15. Sawatzky DA, Willoughby DA, Colville-Nash PR, Rossi AG. The involvement of the apoptosis-modulating proteins ERK 1/2, Bcl-xL and Bax in the resolution of acute inflammation in vivo. Am J Pathol 2006;168:33–41. [PubMed: 16400007]
16. Rossi AG, et al. Cyclin-dependent kinase inhibitors enhance the resolution of inflammation by promoting inflammatory cell apoptosis. Nat Med 2006;12:1056–64. [PubMed: 16951685]

17. Reville K, Crean JK, Vivers S, Dransfield I, Godson C. Lipoxin A4 redistributes myosin IIA and Cdc42 in macrophages: implications for phagocytosis of apoptotic leukocytes. J Immunol 2006;176:1878–1888. [PubMed: 16424219]

18. Freire-de-Lima CG, et al. Apoptotic cells, through transforming growth factor-beta, coordinately induce anti-inflammatory and suppress pro-inflammatory eicosanoid and NO synthesis in murine macrophages. J Biol Chem 2006;281:38376–38384. [PubMed: 17056601]

19. Maderna P, Yona S, Perretti M, Godson C. Modulation of phagocytosis of apoptotic neutrophils by supernatant from dexamethasone-treated macrophages and annexin-derived peptide Ac(2-26). J Immunol 2005;174:3727–3733. [PubMed: 15749912]

20. Liu Y, et al. Glucocorticoids promote nonphlogistic phagocytosis of apoptotic leukocytes. J Immunol 1999;162:3639–46. [PubMed: 10092825]

21. Vandivier RW, Henson PM, Douglas IS. Burying the dead: the impact of failed apoptotic cell removal (efferocytosis) on chronic inflammatory lung disease. Chest 2006;129:1673–1682. [PubMed: 16778289]

22. Underhill DM. Macrophage recognition of zymosan particles. J Endotoxin Res 2003;9:176–180. [PubMed: 12831459]

23. Gilroy DW, et al. Inducible cycloxygenase may have anti-inflammatory properties. Nature Med 1999;5:698–701. [PubMed: 10371510]

24. Gronert K, et al. A role for the mouse 12/15-lipoxygenase pathway in promoting epithelial wound healing and host defense. J Biol Chem 2005;280:15267–15278. [PubMed: 15708862]

25. Sadik CD, Sies H, Schewe T. Inhibition of 15-lipoxygenases by flavonoids: structure-activity relations and mode of action. Biochem Pharmacol 2003;65:773–781. [PubMed: 12628491]

26. Bellingan GJ, et al. Adhesion molecule-dependent mechanisms regulate the rate of macrophage clearance during the resolution of peritoneal inflammation. J Exp Med 2002;196:1515–1521. [PubMed: 12461086]

27. Cao C, Lawrence DA, Strickland DK, Zhang L. A specific role of integrin Mac-1 in accelerated macrophage efflux to the lymphatics. Blood 2005;106:3234–3241. [PubMed: 16002427]

28. Pond CM. Adipose tissue and the immune system. Prostaglandins Leukot Essent Fatty Acids 2005;73:17–30. [PubMed: 15946832]

29. Wellen KE, Hotamisligil GS. Inflammation, stress, and diabetes. J Clin Invest 2005;115:1111–1119. [PubMed: 15864338]

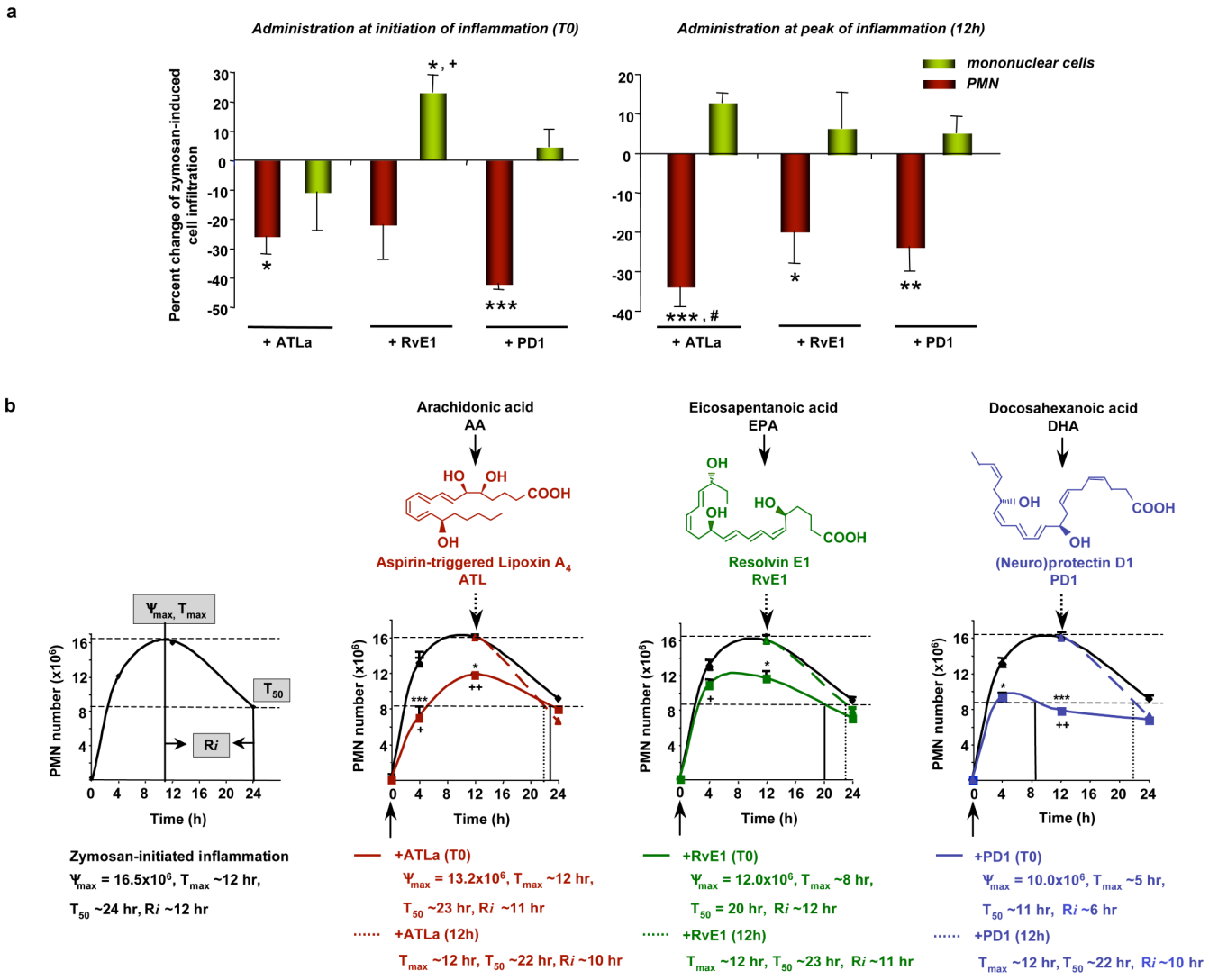

Figure 1. Pro-resolving lipid mediators RvE1, PD1 and ATLa direct local phagocyte tissue flux

(A) Peritonitis. ATLa, RvE1, or PD1 (300 ng, ip) was given either with zymosan (T_0, *left*) or after (12h, *right*), and peritoneal exudates collected (24h). Results are the mean ± s.e.m (n=4-8). **p*<0.05, ***p*<0.01, ****p*<0.001, compared to zymosan alone; ^{+}p<0.05, ATLa vs. RvE1; $^{\#}p$<0.05, T_0 vs. 12h (B) Resolution Indices were defined in [ref. 12] (Supplemental Fig. 1), including ψ_{max} (maximal PMN), T_{max} (time point when PMNs reach ψ_{max}), T_{50} (time point corresponding to ~50% PMN reduction) and R_i (*resolution interval*, the interval between T_{max} and T_{50}). These indices were calculated when compounds were given at the initiation (T_0, solid lines and arrows) or peak (12h, dashed lines and arrows) of inflammation. Results are the mean ± s.e.m. (n=4-8). **p*<0.05, ****p*<0.001, compared to zymosan alone; ^{+}p<0.05, ATLa vs. RvE1; ^{++}p<0.01, ATLa vs. PD1.

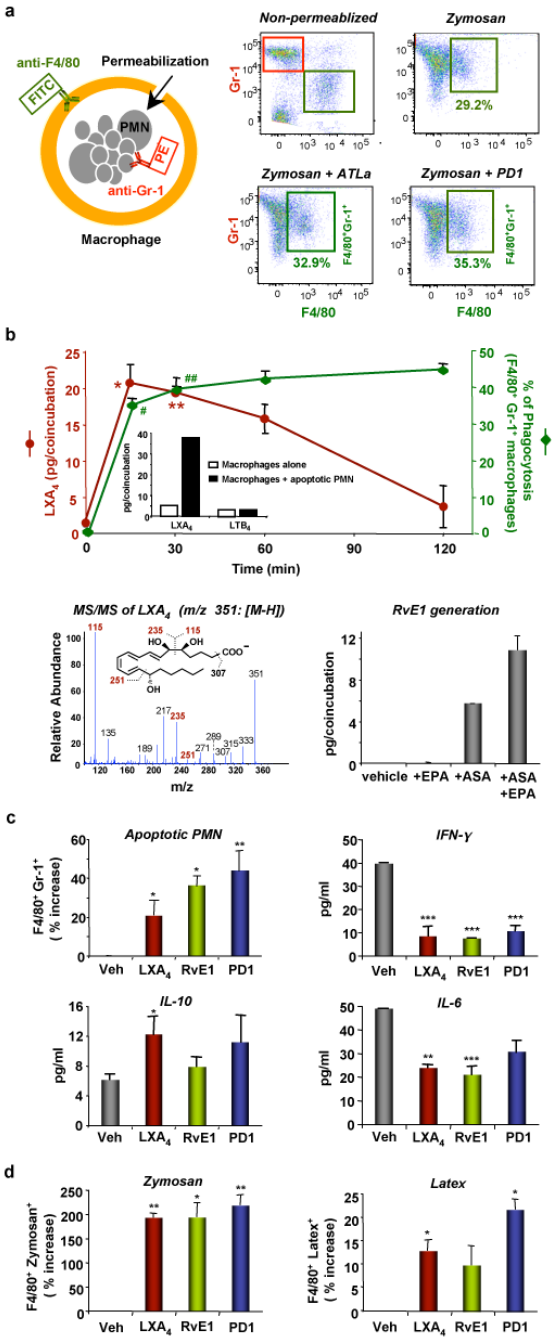

Figure 2. RvE1 and PD1 increase macrophage phagocytic activity *in vivo* and *in vitro*

(A) *In vivo* phagocytosis with representative dot plots of FACS analysis. (B) (*Top*) Time course of eicosanoid generation and phagocytosis activity *in vitro*. Results are the mean ± s.e.m. (n=3). LXA_4 amounts are expressed as pg/coincubation ($0.4x10^6$ PMN+$0.2x10^6$ macrophages in 0.2 ml). **p*=0.01, ***p*=0.02 (vs. time 0 or 120 min). Phagocytosis activities are expressed as [$F4/80^+Gr\text{-}1^+/F4/80^+$]x100%. $^{\#}p$=0.03, $^{\#\#}p$=0.01 (vs. time 120 min). (*Inset*) LXA_4 and LTB_4 generation at 60 min. *(Bottom left)* MS/MS spectrum of LXA_4. (*Bottom right*) RvE1 generation. Macrophages were incubated with ASA (500 μM, 30 min) followed by EPA (20 μM, 45 min) prior to incubation with apoptotic PMN. RvE1 was determined by LC/MS/MS and expressed as pg/coincubation ($2x10^6$ PMN+$1x10^6$ macrophages in 1 ml). (C) Phagocytosis of apoptotic

PMN *in vitro*. Results are the mean ± s.e.m. (n=3-4) and expressed as percent increase of $F4/80^{+}Gr\text{-}1^{+}$ macrophages compared to vehicle alone. Cytokine/chemokine levels are the mean ± s.e.m. (n=3). **p*<0.05, ***p*<0.01, ****p*<0.001, compared to vehicle alone. (D) Phagocytosis of zymosan and latex particles *in vitro*. Results are the mean ± s.e.m. (n=3) and expressed as percent increase of $F4/80^{+}$zymosan^{+} or $F4/80^{+}$latex^{+} macrophages compared to vehicle alone. Results are the mean ± s.e.m. (n=3). **p*<0.05, ***p*<0.01 compared to vehicle alone.

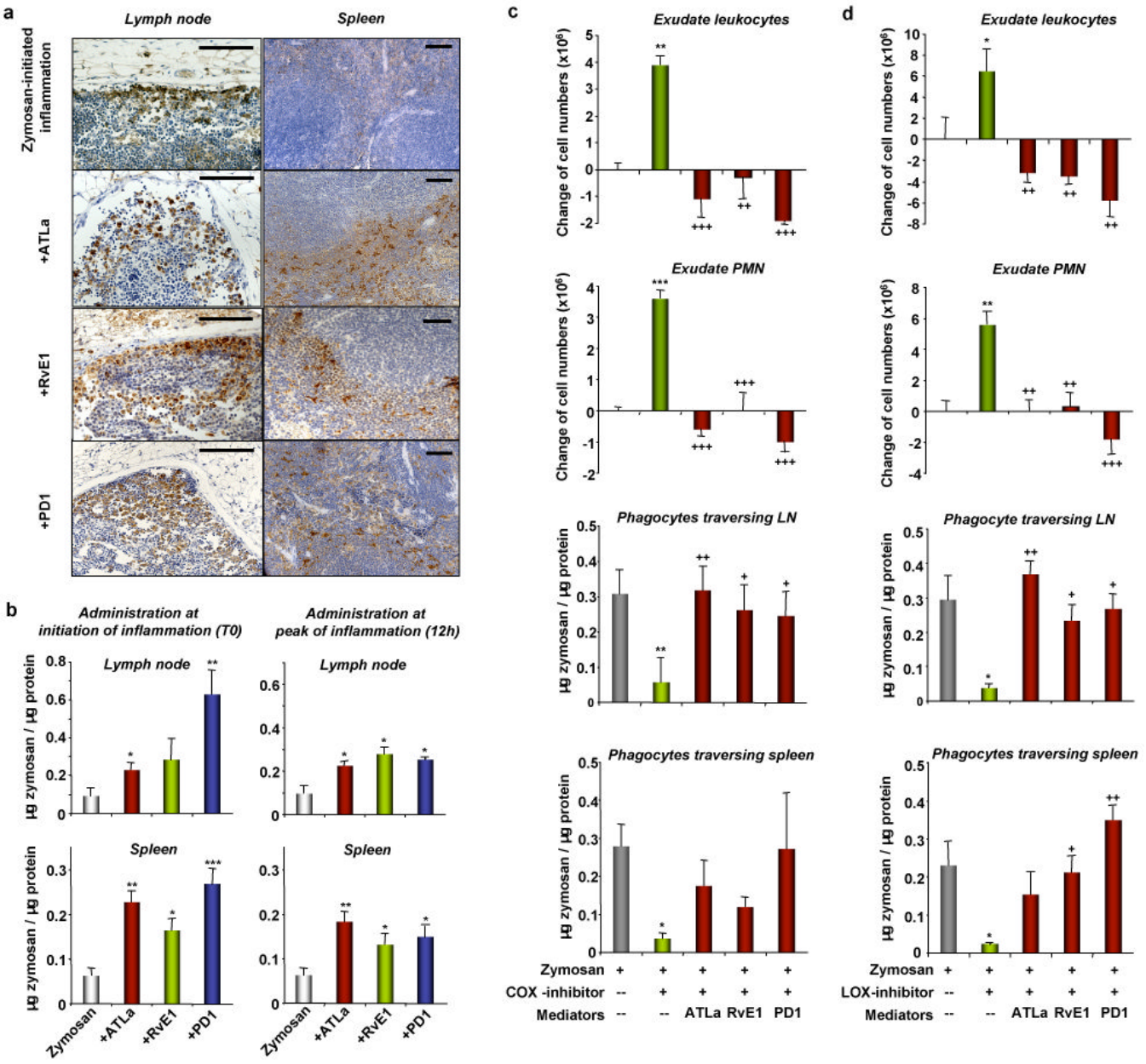

Figure 3. RvE1 and PD1 enhance leukocytes carrying phagocytozed zymosan in lymph nodes and spleen

(A) Leukocytes with engulfed-zymosan particles (zymosan^{e}) in the cortex of the LN and marginal zone of the spleen. The brown particles are positive staining of zymosan. Scale bars: 50 µm. (B) Quantification of zymosan. ATLa, RvE1 or PD1 was given at initiation (T_0) or peak (12 h) of inflammation. Results are mean ± s.e.m. (n=4-8). *p=0.05, **p<0.01, ***p<0.001. (C, D) COX or LOX inhibitor was given 30 min before zymosan challenge with or without mediators. Results are mean ± s.e.m. (n=3-4). *p=0.05, **p<0.01, ***p<0.001, compared with zymosan alone; ^{+}p=0.05, ^{++}p<0.01, ^{+++}p<0.001, compared with (C) zymosan + COX-inhibitor or (D) zymosan + LOX-inhibitor.

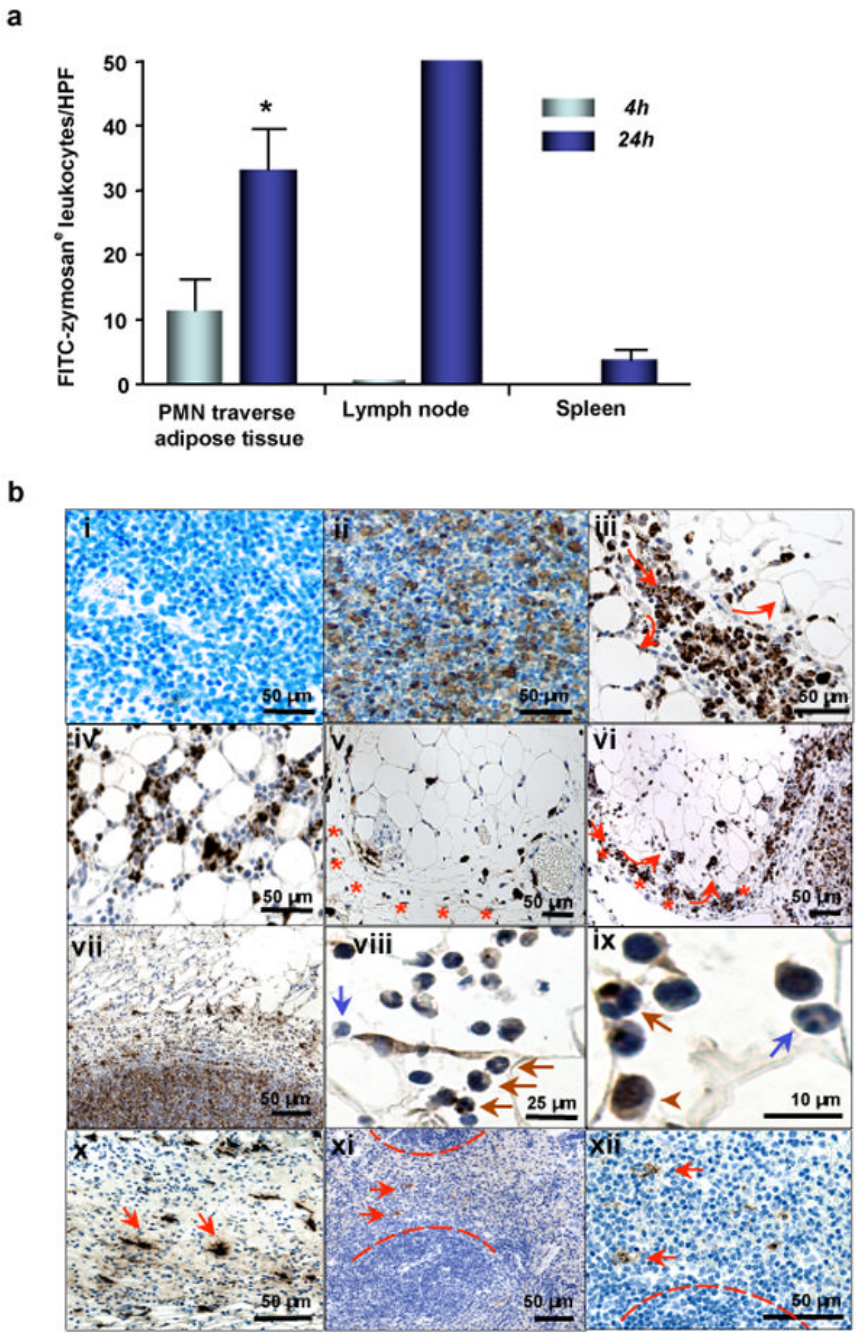

Figure 4. Active removal of leukocytes from the inflammatory exudate

(A) Quantitation of FITC-zymosan^e leukocytes. Results are mean ± s.e.m. (n=3). *p=0.05 (4h vs. 24h). (B) Tracking of FITC-zymosan^e leukocytes 24h after FITC-zymosan injection in the (i) absence or (ii) presence of the primary anti-FITC Ab. The brown particles are positive staining of FITC-zymosan. (iii) Lipopassage (arrows). (iv) Zymosan^e leukocytes in perinodal adipose tissue. (v) In perinodal adipose tissue, lymph vessels (stars) conduct zymosan^e leukocytes in proximity to blood vessels. (vi) Zymosan^e leukocytes in the afferent lymph vessel (stars) and subcapsular sinus. (vii) In the lymph nodes, zymosan^e leukocytes were detected markedly in cortex areas. (viii, ix) Zymosan^e leukocytes consisted of monocytes/macrophages (arrowheads), and non-apoptotic PMNs with engulfed-zymosan (brown arrows) or without

(blue arrows). (x) Dendritic-like (fine cell protrusions), zymosan[e] leukocytes in the afferent lymph vessels (arrows). (xi, xii) In the spleen, some zymosan[e] leukocytes also displaced morphological characteristics of DCs (arrows).